A New Design for Active Isolation of Patient's Compartment from Ambulance Body using the Adaptive Control Method

Aliasqar Meraji
Department of Mechanical Engineering,
Imam Hossein Comprehensive University, Iran
E-mail: AliasqarMeraji@ihu.ac.ir

Saeed Mahjoub Moghadas *
Department of Mechanical Engineering,
Imam Hossein Comprehensive University, Iran
E-mail: smahjoubmoghadas@ihu.ac.ir
*Corresponding author

Received: 21 March 2022, Revised: 03 May 2022, Accepted: 28 June 2022

Abstract Vertical vibrations in the ambulance patient compartment due to road disturbances can cause serious injury to patients. In the present study, after extracting the vibrations entering an ambulance with passive suspension system, the use of a new active vibration isolation system between the patient's Compartment and the ambulance body is proposed. This isolation system includes an air spring, a linear shaft motor and a suitable active controller, which is abbreviated as AVI system. In this paper, instead of using one AVI system to control the vibrations of the stretcher, four AVI systems are used to control the vibrations of the patient's Compartment. The accurate modelling for ambulance with passive suspension system in both types non-isolated and active isolated patient's Compartment has been done by SOLIDWORKS software. Then by extracting the mathematical model, differential equations and state space model, the comparison of both types was done using MATLAB-SIMULINK software and finally the results were optimized using the Model Reference Adaptive Control (MRAC). In this control method, the functional parameters automatically adapt themselves by changing the position of the centre of gravity. The results obtained according to the IS02631 standard, show that with the present method, vertical vibrations are reduced by more than 80%.

Keywords: Active Vibration Isolator, Adaptive Control, Ambulance Suspension System, IS0 2631 Standard, Patient's Compartment

How to cite this paper: Aliasqar Meraji, and Saeed Mahjoub Moghadas, "A New Design for Active Isolation of Patient's Compartment from Ambulance Body using the Adaptive Control Method", Int J of Advanced Design and Manufacturing Technology, Vol. 15/No. 3, 2022, pp. 11-26.
DOI: 10.30486/admt.2022.1942823.1319.

Biographical notes: Aliasqar Meraji is a PhD candidate in Mechanical Engineering at Imam Hossein Comprehensive University, Iran. He received his MSc in Mechatronic Engineering from Islamic Azad University, Bafgh branch in 2014. He is currently working as a researcher in the Aviation Industries. His current research focuses on Vibrations Isolation Theory and modal analysis. **Saeed Mahjoub Moghadas** is Associate Professor of Mechanical Engineering at Imam Hossein Comprehensive University since 1986, Iran. He received his PhD in Mechanical Engineering from Ensam university in Paris, France in 1985. He has authored 20 books and translated 15 others in the field of dynamic, vibration and control.

1 INTRODUCTION

Patient's body is extremely sensitive to sudden impulses, and patient's body vibrations are intolerable in cases where they reach the resonant frequency that is beyond human toleration limit. Ambulances are important in that they not only transport injured patients quickly but are also capable of providing first aid to patients. Many of the patients carried by an ambulance are in serious condition, with brain injuries, cardiac issues and so on. Such patients are particularly sensitive to even small amounts of vibration.

Since the transfer of patient and vibrations entered the ambulance may induce various physiological alterations which may adversely affect the prognosis of the patient, the sensitivity of the patient's body to vibrations should be considered. [1]. Although enhanced roads quality and reduced road disturbances have provided the ground for travel comfort at high velocities, vertical deflections such has speed bumps are installed on roads in an attempt to control the unbridled speed of vehicles. In curved roads, such deflections can cause dangerous vibrations in the patient carrying ambulances. Given that the patients who are transported in ambulances are mostly in acute and severe conditions such as heart surgery, brain and vertebral conditions and new-born babies their body is sensitive to the slightest vibrations [2].

Most patients also believe that the most terrible causes of injury incidence and exacerbation are experienced when route to the nearest medical centre on an ambulance, and attribute this problem to old ambulances [3]. Moreover, Karlsson investigated the effect of in-ambulance medical care on an under 7-year-old kid, his hear analysis and the extent to which his body vibrations exceed the recommended limit [4]. Since ambulances use suspension systems that fit the basic vehicles, they cannot control the vibrations that are exerted to the patient and paramedics' body, thus, attempts are made in several studies to attenuate such vibrations. In most of these studies, the approach to attenuation of vibrations in patients' body is mostly focused on the stretcher system [5].

Abd-El-Tawwab investigated the Vertical vibration damping through a low-speed active isolation system for a stretcher with hydrodynamic dampers [6]. Henderson and Raine investigated a suspensions system that introduced a semi-active pneumatic damper within a stretcher system [7-8], Raemaekers minimized the vibrations applied to the patient by isolating the stretcher from the body of the ambulance patient's compartment by an active isolation system. The system was a combination of pneumatic and electromagnetic forces to reduce vertical forces.

He was able to optimize the active vibration isolation system by creating a quarter car model of an ambulance and using a Skyhook controller. Finally, the isolation results provided patient comfort conditions in accordance with ISO 2631 [9]. Niu Fu et al also conducted an experimental study on a vibration isolator system for an ambulance stretcher using a spring and plastic-metal structure.

In this system, he also investigated the comfort standards for patients in lying position and vibrations exerted to all organs when the ambulance is moving along asphalt, rail, and dirt roads at the velocity range of 10-80 km/h and showed that the acceleration exerted to patients in these roads ranges from 0.0316 m/s² to 1.216 m/s², which is indicative of patients' discomfort. Using this mechanism, he managed to attenuate this acceleration and reduce the vibrations exerted from ambulance compartment to the stretcher, by 17 to 47% [10]. It should be noted that, the previous studies only cover the measures taken to attenuate the stretcher vibrations, and do not deal with attenuation of vibrations exerted to patient and paramedics.

By isolating the bed stage from the ambulance body using four Magnetorheological dampers installed in four comers of the bed stage, Choi and Chae managed to propose a model that could attenuate the vibrations that patients and paramedics are exerted to in the ambulance and provide them with comfort when the ambulance moved along different winding roads or over speed bumps. Using the sliding mode controller and by measuring the stimulus signal using accelerometers, they managed to create the damping force of the MR dampers. They also used the full-scale vehicle model to obtain the control equations [11].

Hengmin Qi et al selected a typical sport utility vehicle with 10 degrees of freedom to conduct the dynamic simulation, the results indicated that, by controlling hydraulically interconnected suspension key parameters, the vehicle dynamic performance can be effectively controlled in both roll and lateral planes [12]. Fialho and Balas introduced a road adaptive control design for active suspension systems, which includes two levels of adaptation that are based on the nonlinear characteristics of the suspension system and the road conditions, respectively [13]. Motivated by the desirable performance of the model reference adaptive control (MRAC) approach, various literature studies have investigated its performance in diverse linear and nonlinear practical systems [14-15]. Drawing on the previous experiences and investigations, in the present study, the main purpose of this study is to isolate the patient's compartment from the body and the passive suspension system of the ambulance, which is achieved by installing four active vibration isolation systems in the lower four corners of the compartment (“Fig. 1”).

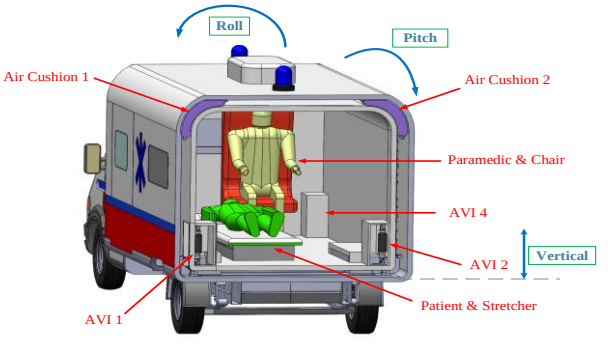

Fig. 1 Layout of the proposed patient's Compartment isolated from the ambulance body by an AVI system and the location of air cushion.

This system is designed based on the combination of pneumatic and electromagnetic forces associated with the ambulance data. After developing the full-scale model of the ambulance equipped with the passive suspension system and developing a dynamic model for that, the equations used to calculate the forces exerted on the wheels when the vehicle is passing curved roads or speed bumps will be obtained.

In addition, the obtained data were used to calculate the forces exerted on the edges of the isolated part in the patient compartment in order to design the AVI system. Given that AVI system is of great importance in the dynamic equations, the ambulance data, and ambulance limitations in general, and the patient compartment limitations in particular were used to develop the isolated part of the patient compartment along with the AVI systems.

Moreover, the adjustable air cushions were installed in the top comers of the vehicle between the patient compartment and the ambulance ceiling in order to contribute to the AVI system performance and develop the passive compartment model when the patient compartment is vacant.

In other words, this model allows for activation and deactivation of the above-mentioned system in the patient compartment. When in motion, all vehicles have three main control movements: z axis is along the vertical axis of the vehicle (z), Roll is the rotation of a vehicle about the longitudinal axis (ø) and Pitch is the rotation of a vehicle about the transverse axis (θ). And this also holds true for the ambulance in this study. Since four AVI systems are installed at the comers of the isolated part in the patient compartment, 4 active actuators'(Flm1, Flm2, Flm3, and Flm4) need to be designed to control the effect of the three main vibrational motions. To this end, the conventional vibration control techniques are used for performance evaluation purposes.

2 DESIGNING AN ACTIVE VIBRATION ISOLATOR SYSTEM

The AVI system is supposed to tolerate heavy weights and develop the required active dynamic and static forces as well as adjustable reciprocating moves. Power consumption in this system is negligible compared to other systems. The required static force must offset the allowed load on the AVI system, and the active dynamic force must accomplish the isolation process by generating effective and adjustable reciprocating moves. Moreover, the guide system must be free from any friction or backlash effect so that the system can function properly. Thus, in the present study a customized air spring that meets the linear conditions and tolerates heavy weights at the same time, is used to supply the required static force.

This absorber is preferred over hydraulic systems and conventional old springs that had some intrinsic disadvantages such as backlash as well as relatively high weight and stiffness. The electromagnetic motor was selected, from among a variety of oilier options, in order to generate the active dynamic reciprocating move. The advantages of this motor include: low stiffness (near zero), friction-less function, extremely high band-width and low energy dissipation. This actuator is a linear shaft motor or an electromagnetic motor with non-cylindrical stator that generates a linear force, rather than rotational moment, along the stator.

This linear shaft motor includes a set of moveable coils that surround the magnetic shaft (forcer). The magnetic field around the shaft is not transferred to other areas. In such motors, the forcer can use the maximum magnetic current, therefore the air gap between the forcer and shaft is not critical (within the 0.5 to 1.75 mm). These motors take full advantage of magnetic current and do not need to be cooled down, that's why they do not include additional parts. Moreover, they do not have any backlash or vibration which makes them very effective.

The linear shaft motor is equipped with an analogue hall encoder.

This encoder is used to feedback locations to the controller. Therefore, in order to optimally design an AVl system that is composed of a set of air springs, linear shaft motors and guidance systems, it is necessary to design the air spring according to the weight and road inputs it is supposed to tolerate and select an electromagnetic motor that fits the air spring. The force dial created by the air spring is used to eliminate the static force of the isolated patient compartment and maintain its balance. The electromagnetic force of the linear shaft motor is used for rapid reaction to vertical forces and modification of air spring force variations.

Therefore, in order to determine the forces exerted to the AVI system, it is necessary to specify the location of this system in the Ambulance vehicles used in Iran (Sprinter 314 GIFA). Since, the location of AVl systems is of great importance in dynamic equations, the SolidWorks modeling software has been used to design AVI systems and their installation position in the four corners of the compartment. Distances and location of AVI systems were designed according to the sizes that had already been specified in the ambulance construction plan. The transversal and longitudinal distance between two AVI systems is 1441mm and 2959.5 mm respectively. The distance between the AVl system in the rear part of the patient room and rear axle of the ambulance is 813 mm, while the distance between the AVl system in the front part of the patient compartment and the front axle of the vehicle is 1406 mm.

After the isolation process, the patient compartment underwent some formal changes and its layout in the simulated model was specified (See "Fig. 1"). The centre of gravity will be of great importance in the dynamic model that will be required in the following stages. Therefore, in order to determine the centre of gravity, it is necessary to specify the weight of patient compartment including the weight of patient, paramedic, the compartment body, the stretcher and other accessories. The body of van compartments is usually made of Acrylonitrile butadiene styrene or propylene. The selected polymer for designing the compartment in the present study was Acrylonitrile butadiene styrene. After selection of this polymer in the simulation software, the weight of this compartment was equal to 925 kg. assuming that the a typical individual and stretcher weigh about 80 kg and 20 kg, respectively, die total weight obtained for the patient compartment was 1105 kg.

Air spring stiffness is one of the most important design features of the AVI system design. According to the above-mentioned information, it can be argued that die rigidness of the air spring is equal to the force required for shrinkage or expansion of the air spring per its height unit. Thus, the air spring stiffness can be calculated using "Eq. (1) " .

$$K_a = \frac{\gamma p_0 A_c^2}{V_0} = \frac{\gamma mg\, A_c}{V_0} \quad (1)$$

In this equation, the air spring is designed in accordance with the required displacement stroke and the weight it is supposed to tolerate. The stroke of this spring is simulated based on passage of the ambulance over different speed bumps such as Watt profile with the height of 100 mm (See "Fig. 2"). The maximum displacement stroke will be about 15 cm and the linear shaft motor should also feature the same displacement stroke [9]. In "Eq. (1)" , weight of each air spring is equal to 0.25 of the total patient compartment weight and since the patient compartment mass was assumed to be 1105 kg, the mass of each air spring is equal to 276.25 kg in the static mode. A linear shaft motor will be embedded within each air spring in such a way that the net air volume is reduced in proportion to the volume of the linear shaft motor.

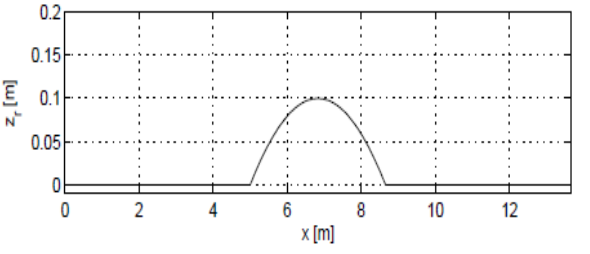

Fig. 2 Speed bump with Watt profile.

Considering that the air hole volume is equal to 0.00724994 mm³, the effective air space based on the air spring's dimensions will be 0.016587658 mm², and the stiffness coefficient of the air spring, obtained from the "Eq. (1) " will be equal to 8680.6 N/m.

$$f_n = \frac{1}{(2\pi)\sqrt{\rho g A V_0}} \quad (2)$$

According to "Eq. (2) " , the resonance frequency is equal to 3.91Hz. Since the highest vibration sensitivity range in human body is 4-8 Hz, and the actuator's bandwidth must be below this frequency range, actuator would be a suitable choice in this case. The required electromagnetic force of the active system is to a great extent dependent on the actuator's stroke and the air spring stiffness. For example, in simulation of Watt profile according to "Eq. (3)", the minimum required force of the linear shaft motor is equal to 1.3 kN.

$$k_a \times Stroke = F_{lm} = 8680.6 \times 0.15 = 1302.09\ N \quad (3)$$

The selected linear shaft motor is of XTB3808 type and its parameters and values are listed in "Table 1" .

Table 1 The XTB3808 Linear Shaft Motor specifications

Specifications	Unit	Value
Peak Force	(N)	1488
Continuous stall Force	(N)	232.1
Peak Acceleration	(m/s²)	295
Maximum Speed	(m/s)	3.5
Maximum stroke	(mm)	1219
Forcer Mass	(kg)	5.05
Thrust rod mass/meter	(kg/m)	8.3
Rod diameter	(mm)	38

The guiding system is composed of three guiding wheels that are assembled on a linear shaft motor at an angle of 120 degrees and in case they are loaded properly, they can bring about an appropriate guidance with minimum friction. Two wheels are fixed and the third one is firmly pressed against the shaft by a spring. This pre-tension assures that all the wheel are continuously in contact and thus backlash will he avoided. The shaft of the linear motor is made of stainless steel and the wheels are made of Polyoxymethylene that has a low modulus of elasticity ($E2$=2.8 GPa) compared to steel (E= 210 GPa) and therefore the contact stress will be lower when POM wheels are used instead of steel wheels. Figure 3 shows the location of these wheels and three displacement strokes of the assembled AVI system.

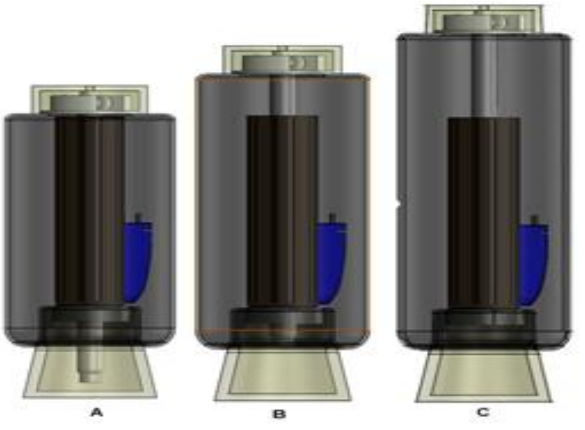

Fig. 3 Three displacement strokes of the assembled AVI system where the guiding system and the selected linear shaft motor are embedded within a customized air spring.

3 INVESTIGATION OF PASSIVE SUSPENSION SYSTEM IN OF THE AMBULANCE

3.1. Motion Equations and the State Space Model

In the present study, the ambulance selected in Iran has a passive suspension system. According to the Sprinter 314 user manual, the position of the center of gravity and the distance between the road disturbances force input and center of gravity are available. These positions and distances are shown in "Table 2" .

Table 2 The longitudinal and transversal distances to Ambulance CG –without isolation of patient's Compartment

Specifications	Unit	Value
a1	(mm)	3281
b1	(mm)	1082.75
c1	(mm)	712
d1	(mm)	714

The state space model of the ambulance motion equations with passive suspension in both types of non-isolated and active isolated patient's compartment can be used to understand the level of discomfort for patients and paramedics. According to Newton's second law and the mechanical model of the ambulance presented in "Fig. 4" , which has 7 degrees of freedom, "Eqs. (4-10)" are obtained.

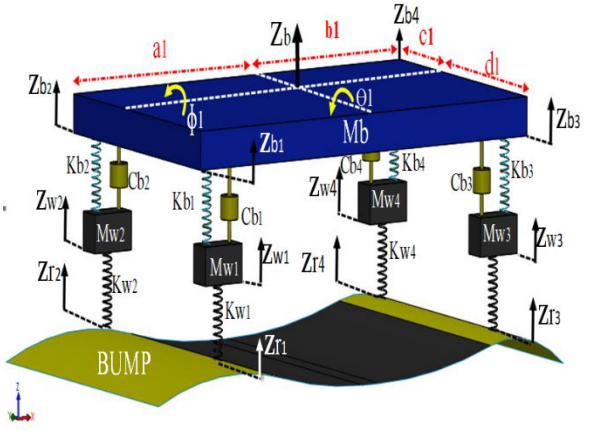

Fig. 4 Mechanical model of the ambulance with passive suspension system and non-isolated patient's compartment.

$$\begin{aligned}\ddot{Z}_{w1} = {} & K_{b1}(Z_{b1} - Z_{w1}) + C_{b1}(\dot{Z}_{b1} - \dot{Z}_{w1}) \\ & - K_{w1}(Z_{w1} - Z_{r1}) \\ & - K_{b1}(a_1 - e_1)\theta_1 \\ & - C_{b1}(a_1 - e_1)\dot{\theta}_1 \\ & + K_{b1}(d_1\varphi_1) + C_{b1}(d_1\dot{\varphi}_1)\end{aligned} \tag{4}$$

$$\begin{aligned}M_{w2}\ddot{Z}_{w2} = {} & K_{b2}(Z_{b2} - Z_{w2}) \\ & + C_{b2}(\dot{Z}_{b2} - \dot{Z}_{w2}) \\ & - K_{w2}(Z_{w2} - Z_{r2}) \\ & - K_{b2}(a_1 - e_1)\theta_1 \\ & - C_{b2}(a_1 - e_1)\dot{\theta}_1 \\ & + K_{b2}(c_1\varphi_1) + C_{b2}(c_1\dot{\varphi}_1)\end{aligned} \tag{5}$$

$$\begin{aligned}M_{w3}\ddot{Z}_{w3} = {} & K_{b3}(Z_{b3} - Z_{w3}) \\ & + C_{b3}(\dot{Z}_{b3} - \dot{Z}_{w3}) \\ & - K_{w3}(Z_{w3} - Z_{r3}) \\ & + K_{b3}(b_1\theta_1) + C_{b3}(b_1\dot{\theta}_1) \\ & + K_{b3}(d_1\varphi_1) + C_{b3}(d_1\dot{\varphi}_1)\end{aligned} \tag{6}$$

$$\begin{aligned}M_{w4}\ddot{Z}_{w4} = {} & K_{b4}(Z_{b4} - Z_{w4}) \\ & + C_{b4}(\dot{Z}_{b4} - \dot{Z}_{w4}) \\ & - K_{w4}(Z_{w4} - Z_{r4}) \\ & + K_{b4}(b_1\theta_1) + C_{b4}(b_1\dot{\theta}_1) \\ & - K_{b4}(c_1\varphi_1) - C_{b4}(c_1\dot{\varphi}_1)\end{aligned} \tag{7}$$

$$
\begin{aligned}
M_b\ddot{Z}_b = &-K_{b1}(Z_{b1}-Z_{w1})\\
&-C_{b1}\left(\dot{Z}_{b1}-\dot{Z}_{w1}\right)\\
&-K_{b2}(Z_{b2}-Z_{w2})\\
&-C_{b2}\left(\dot{Z}_{b2}-\dot{Z}_{w2}\right)\\
&-K_{b3}(Z_{b3}-Z_{w3})\\
&-C_{b3}\left(\dot{Z}_{b3}-\dot{Z}_{w3}\right)\\
&-K_{b4}(Z_{b4}-Z_{w4})\\
&-C_{b4}\left(\dot{Z}_{b4}-\dot{Z}_{w4}\right)\\
&+K_{b1}(a_1-e_1)\theta_1\\
&+C_{b1}(a_1-e_1)\dot{\theta}_1\\
&+K_{b2}(a_1-e_1)\theta_1\\
&+C_{b2}(a_1-e_1)\dot{\theta}_1\\
&-K_{b3}(b_1\theta_1)-C_{b3}\left(b_1\dot{\theta}_1\right)\\
&-K_{b4}(b_1\theta_1)-C_{b4}\left(b_1\dot{\theta}_1\right)\\
&-K_{b1}(d_1\varphi_1)-C_{b1}(d_1\dot{\varphi}_1)\\
&+K_{b2}(c_1\varphi_1)+C_{b2}(c_1\dot{\varphi}_1)\\
&-K_{b3}(b_1\varphi_1)-C_{b3}(d_1\dot{\varphi}_1)\\
&+K_{b4}(c_1\varphi_1)+C_{b4}(c_1\dot{\varphi}_1)
\end{aligned}
\tag{8}
$$

$$
\begin{aligned}
I_{yy}\ddot{\theta}_1 = &\left[K_{b1}(Z_{b1}-Z_{w1})(a_1-e_1)\right.\\
&+C_{b1}\left(\dot{Z}_{b1}-\dot{Z}_{w1}\right)(a_1\\
&-e_1)-K_{b1}(a_1-e_1)^2\theta_1\\
&\left.-C_{b1}(a_1-e_1)^2\dot{\theta}_1\right]\\
&+\left[K_{b2}(Z_{b2}-Z_{w2})(a_1\right.\\
&-e_1)\\
&+C_{b2}\left(\dot{Z}_{b2}-\dot{Z}_{w2}\right)(a_1\\
&-e_1)-K_{b2}(a_1-e_1)^2\theta_1\\
&\left.-C_{b2}(a_1-e_1)^2\dot{\theta}_1\right]\\
&+\left[-K_{b3}(Z_{b3}-Z_{w3})b_1\right.\\
&-C_{b3}\left(\dot{Z}_{b3}-\dot{Z}_{w3}\right)b_1\\
&-K_{b3}(b_1)^2\theta_1\\
&\left.-C_{b3}(b_1)^2\dot{\theta}_1\right]\\
&+\left[-K_{b4}(Z_{b4}-Z_{w4})b_1\right.\\
&-C_{b4}\left(\dot{Z}_{b4}-\dot{Z}_{w4}\right)b_1\\
&-K_{b4}(b_1)^2\theta_1\\
&\left.-C_{b4}(b_1)^2\dot{\theta}_1\right]
\end{aligned}
\tag{9}
$$

$$
\begin{aligned}
I_{xx}\ddot{\varphi}_1 = &\left[-K_{b1}(Z_{b1}-Z_{w1})d_1\right.\\
&-C_{b1}\left(\dot{Z}_{b1}-\dot{Z}_{w1}\right)d_1\\
&-K_{b1}(d_1)^2\varphi_1\\
&\left.-C_{b1}(d_1)^2\dot{\varphi}_1\right]\\
&+\left[K_{b2}(Z_{b2}-Z_{w2})c_1\right.\\
&-C_{b2}\left(\dot{Z}_{b2}-\dot{Z}_{w2}\right)c_1\\
&-K_{b2}(c_1)^2\varphi_1\\
&\left.-C_{b2}(c_1)^2\dot{\varphi}_1\right]\\
&+\left[-K_{b3}(Z_{b3}-Z_{w3})d_1\right.\\
&-C_{b3}\left(\dot{Z}_{b3}-\dot{Z}_{w3}\right)d_1\\
&-K_{b3}(d_1)^2\varphi_1\\
&\left.-C_{b3}(d_1)^2\dot{\varphi}_1\right]\\
&+\left[K_{b4}(Z_{b4}-Z_{w4})c_1\right.\\
&-C_{b4}\left(\dot{Z}_{b4}-\dot{Z}_{w4}\right)c_1\\
&-K_{b4}(c_1)^2\varphi_1\\
&\left.-C_{b4}(c_1)^2\dot{\varphi}_1\right]
\end{aligned}
\tag{10}
$$

Other parameters used in simulation process and in the state space mode, can be seen in "Eqs. (11-18)".

$$Z_{b1} = -(a_1-e_1)\theta_1 + d_1\varphi_1 + Z_b \tag{11}$$

$$\dot{Z}_{b1} = -(a_1-e_1)\dot{\theta}_1 + d_1\dot{\varphi}_1 + \dot{Z}_b \tag{12}$$

$$Z_{b2} = -(a_1-e_1)\theta_1 - c_1\varphi_1 + Z_b \tag{13}$$

$$\dot{Z}_{b2} = -(a_1-e_1)\dot{\theta}_1 - c_1\dot{\varphi}_1 + \dot{Z}_b \tag{14}$$

$$Z_{b3} = b_1\theta_1 + d_1\varphi_1 + Z_b \tag{15}$$

$$\dot{Z}_{b3} = b_1\dot{\theta}_1 + d_1\dot{\varphi}_1 + \dot{Z}_b \tag{16}$$

$$Z_{b4} = b_1\theta_1 - c_1\varphi_1 + Z_b \tag{17}$$

$$\dot{Z}_{b4} = b_1\dot{\theta}_1 - c_1\dot{\varphi}_1 + \dot{Z}_b \tag{18}$$

The open-loop state space form is developed according to "Eqs. (4-18)".

$$
\begin{aligned}
\dot{X}(t) &= Ax(t) + Bu(t)\\
Y(t) &= Cx(t) + Du(t)
\end{aligned}
\tag{19}
$$

According to "Eq. (19)", in the state space model, A is the "state (or system) matrix" (n×n), B is the "input matrix" (n×m), and C is the "output matrix" (r×n), D is the "feedthrough (or feedforward) matrix" (in cases where the system model does not have a direct feedthrough, D is the zero matrix (r×m), According to seven dynamic equations, we will have 14 state variables (n=14).

Defining the state variables of passive suspension system: $X_1 = Z_{w11}$, $X_2 = \dot{Z}_{w1}$, $X_3 = Z_{w2}$, $X_4 = \dot{Z}_{w2}$, $X_5 = Z_{w3}$, $X_6 = \dot{Z}_{w3}$, $X_7 = Z_{w4}$, $X_8 = \dot{Z}_{w4}$, $X_9 = Z_b$, $X_{10} = \dot{Z}_b$, $X_{11} = \theta_1$, $X_{12} = \dot{\theta}_1$, $X_{13} = \varphi_1$, $X_{14} = \dot{\varphi}_1$.

The road roughness will serve as 4 inputs of the ambulance suspension system (m=4), that are introduced into the wheels (Z_{w_1}, Z_{w_2}, Z_{w_3}, Z_{w_4}). This system has 6 outputs (r=6). Defining the outputs of passive suspension system: $Y_1 = X_9$, $Y_2 = X_{10}$, $Y_3 = X_{11}$, $Y_4 = X_{12}$, $Y_5 = X_{13}$, $Y_6 = X_{14}$.

The state space equations of passive suspension system are obtained: $\dot{X}_1 = X_2$, $\dot{X}_2 = \ddot{Z}_{w1}$, $\dot{X}_3 = X_4$, $\dot{X}_4 = \ddot{Z}_{w2}$, $\dot{X}_5 = X_6$, $\dot{X}_7 = X_8$, $\dot{X}_8 = \ddot{Z}_{w4}$, $\dot{X}_9 = X_{10}$, $\dot{X}_{10} = \ddot{Z}_b$, $\dot{X}_{11} = X_{12}$, $\dot{X}_{12} = \ddot{\theta}_1$, $\dot{X}_{13} = X_{14}$, $\dot{X}_{14} = \ddot{\varphi}_1$ and Finally Matrices A, B and C are obtained through the state space equations.

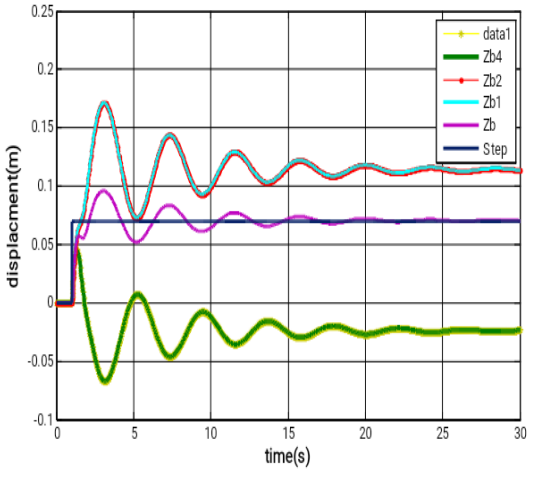

Fig. 6 The response of the passive suspension system of an ambulance with non-isolated patient's compartment to the Step profile input: (a): vertical displacement, and (b): vertical acceleration.

3.2. Investigation of the Passive Suspension System Response to Different Inputs

In order to investigate a suspension system, first we should check its inputs. Road-induced disturbances are introduced in form of sine waves, step functions, or specific road profiles such as Watt, Step and... Thus, investigation of the system response to such inputs is of vital importance in this case. In investigation of system responses, it should always be noted that a favorable system has two main features:

1- It does not experience irritating vibrations or jolts, in other words, it has an acceptable overshoot level.

2- It has a very low setting time; in other words, it eliminates the vibration soon and helps the vehicle get back to the stable and ideal state.

Therefore, in this investigation, two widely-used inputs known as Step and Watt profile are examined in the simulation process. The outputs to be examined here include vertical displacement, rotation round the X axis [Roll-Ø] and rotation round the Y axis [Pitch-θ]. That are derived from introduction of road-induced inputs into the suspension system of the ambulance. The results obtained from the Step input and Watt profile are presented in "Figs. 6-7" .

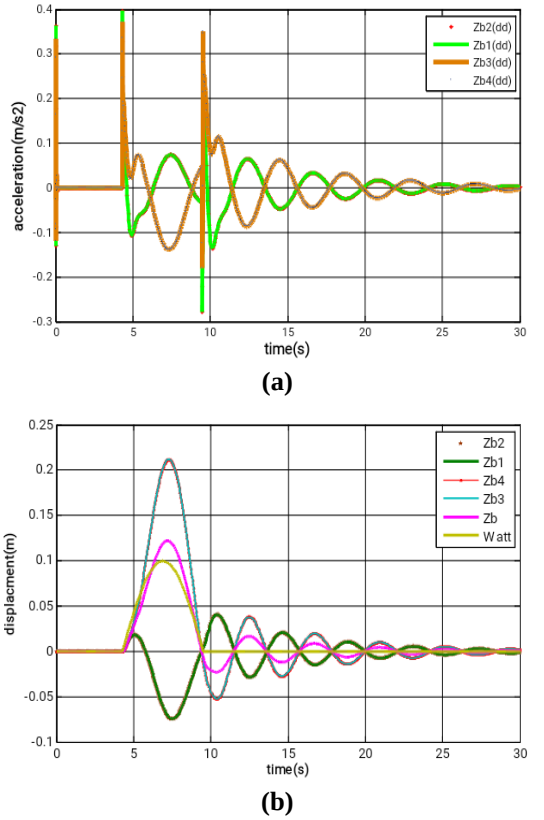

Fig. 7 The response of the passive suspension system of an ambulance with non-isolated patient's compartment to the Watt profile input: (a): vertical displacement, and (b): vertical acceleration.

According to diagrams (b) in "Figs. 6-7" , as well as the scale of discomfort (suggested by IS0 2631 standard) in "Table 4" , it can be argued that in the step input the highest and lowest accelerations are 12.5 and -3.5 m/s² that stand in the "extremely uncomfortable".

Table 4 Scale of travel comfort suggested by *ISO 2631*

Acceleration [*m/s²*]	Scale of discomfort
Less than 0.315	Not uncomfortable
0.315 - 0.03	A little uncomfortable
0.5 - 1	Fairly uncomfortable
0.8 - 1-6	Uncomfortable
1.25 - 2.5	Very uncomfortable
Larger than 2	Extremely uncomfortable

The highest and lowest accelerations in the Watt profile are 0/4 and -2.8 m/s², respectively that stand in the "a little uncomfortable" acceleration range according to the same criterion. Hence it can be argued that the suspension system in this ambulance exerts a highly accelerated vertical force to the individuals in the patient compartment and may cause discomfort or injury when the vehicle is in motion. In addition, vertical displacement resulting from the forces is relatively high during their setting time, but the range of rotation around the X and Y axes is very negligible. Thus, the ineffectiveness of this suspension system, especially in terms of vertical forces exerted to the patient, is proved and it is deemed necessary to modify the structure of this system in order to provide the patient with a comfortable travel along with critical cares.

4 INVESTIGATIONS OF RESPONSES TO THE ACTIVE ISOLATED PATIENT'S COMPARTMENT

According to "Fig. 8" , it can be argued that the patient compartment has been isolated by four AVI systems and the analysable dynamic model of each AVI system has been replaced with a spring, a damper and an actuator so that their parameters are denoted by *Ka*, *Ca*, *Flm* respectively.

The numerical values of the model parameters are provided in "Table 3" . The dynamic equation of the new system is the same as the passive system equations except that the patient compartment and its rotation around the X and Y axes have added three additional equations to the system. However, the impact of patient compartment on the equations of passive suspension system should not be overlooked.

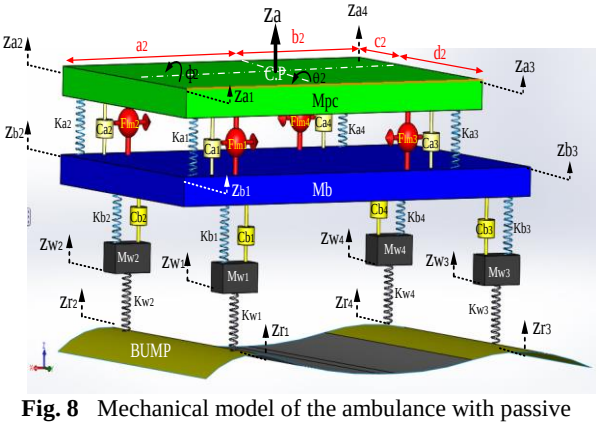

Fig. 8 Mechanical model of the ambulance with passive suspension system and active isolated patient's compartment (with four AVI).

Table 3 Mechanical properties related to the ambulance motion equations with passive suspension system in both types: non-isolated patient's Compartment and active isolated patient's Compartment

Parameters	Unit	Value
Mt	(kg)	3500
Mb	(kg)	2395
Mpc	(kg)	1105
Kb1=Kb2	(kN/m)	24
Cb1=Cb2	(Ns/m)	4200
Kb= (2Kb1+2Kb3)	(kN/m)	88
Kb3=Kb4	(kN/m)	20
Cb3=Cb4	(Ns/m)	2500
Mw	(kg)	60
Kw3=Kw4	(kN/m)	287
Kw1=Kw2	(kN/m)	446
Ka 1,2,3,4	(N/m)	8680.6
Ca 1,2,3,4	(Ns/m)	10

Finally, the added and modified equations are as follows:

$$
\begin{aligned}
M_b\ddot{Z}_b = {} & The\ right\ side\ of\ the\ "Eq.(8)" \\
& + K_{a1}(Z_{a1} - Z_{b1}) \\
& + C_{a1}(\dot{Z}_{a1} - \dot{Z}_{b1}) \\
& + K_{a2}(Z_{a2} - Z_{b2}) \\
& + C_{a2}(\dot{Z}_{a2} - \dot{Z}_{b2}) \\
& + K_{a3}(Z_{a3} - Z_{b3}) \\
& + C_{a3}(\dot{Z}_{a3} - \dot{Z}_{b3}) \\
& + K_{a4}(Z_{a4} - Z_{b4}) \\
& + C_{a2}(\dot{Z}_{a4} - \dot{Z}_{b4}) - F_{lm1} \\
& - F_{lm2} - F_{lm3} - F_{lm4}
\end{aligned}
\qquad (20)
$$

$$\begin{aligned} M_{pc}\ddot{Z}_a = &-K_{a1}(Z_{a1}-Z_{b1}) - C_{a1}(\dot{Z}_{a1}-\dot{Z}_{b1}) \\ &+ F_{lm1} - K_{a2}(Z_{a2}-Z_{b2}) \\ &- C_{a2}(\dot{Z}_{a2}-\dot{Z}_{b2}) + F_{lm2} \\ &- K_{a3}(Z_{a3}-Z_{b3}) \\ &- C_{a3}(\dot{Z}_{a3}-\dot{Z}_{b3}) + F_{lm3} \\ &- K_{a4}(Z_{a4}-Z_{b4}) \\ &- C_{a4}(\dot{Z}_{a4}-\dot{Z}_{b4}) + F_{lm4} \\ &+ K_{a1}(a_2\theta_2) + C_{a1}(a_2\dot{\theta}_2) \\ &+ K_{a2}(a_2\theta_2) + C_{a2}(a_2\dot{\theta}_2) \\ &- K_{a3}(b_2\theta_2) - C_{a3}(b_2\dot{\theta}_2) \\ &- K_{a4}(b_2\theta_2) - C_{a4}(b_2\dot{\theta}_2) \\ &- K_{a1}(d_2\varphi_2) - C_{a1}(d_2\dot{\varphi}_2) \\ &+ K_{a2}(c_2\varphi_2) + C_{a2}(c_2\dot{\varphi}_2) \\ &- K_{a3}(d_2\varphi_2) - C_{a3}(d_2\dot{\varphi}_2) \\ &+ K_{a4}(c_2\varphi_2) + C_{a4}(c_2\dot{\varphi}_2) \end{aligned} \tag{21}$$

$$\begin{aligned} &I_{yy}\ddot{\theta}_1 \\ &= The\ right\ side\ of\ the\ \text{“}Eq.\ (9)\text{”} \\ &-[K_{a1}(Z_{a1}-Z_{b1})a_1 + C_{a1}(\dot{Z}_{a1}-\dot{Z}_{b1})a_1 \\ &+ F_{lm1}(a_1) + K_{a1}(a_1)^2\theta_1 + C_{a1}(a_1)^2\dot{\theta}_1] \\ &-[K_{a2}(Z_{a2}-Z_{b2})a_1 + C_{a2}(\dot{Z}_{a2}-\dot{Z}_{b2})a_1 \\ &+ F_{lm2}(a_1) + K_{a2}(a_1)^2\theta_1 + C_{a2}(a_1)^2\dot{\theta}_1] \\ &+[K_{a3}(Z_{a3}-Z_{b3})(b_{1-}e_2) \\ &+ C_{a3}(\dot{Z}_{a3}-\dot{Z}_{b3})(b_{1-}e_2) \\ &+ F_{lm3}(b_{1-}e_2) - K_{a3}(b_{1-}e_2)^2\theta_1 \\ &- C_{a3}(b_{1-}e_2)^2\dot{\theta}_1] \\ &+[K_{a4}(Z_{a4}-Z_{b4})(b_{1-}e_2) \\ &+ C_{a4}(\dot{Z}_{a4}-\dot{Z}_{b4})(b_{1-}e_2) \\ &+ F_{lm4}(b_{1-}e_2) - K_{a4}(b_{1-}e_2)^2\theta_1 \\ &- C_{a4}(b_{1-}e_2)^2\dot{\theta}_1] \end{aligned} \tag{22}$$

$$\begin{aligned} I_{xx}\ddot{\varphi}_1 = &\ The\ right\ side\ of\ the\ \text{“}Eq.\ (10)\text{”} \\ &-[K_{a1}(Z_{a1}-Z_{b1})d_1 \\ &+ C_{a1}(\dot{Z}_{a1}-\dot{Z}_{b1})d_1 \\ &+ F_{lm1}(d_1) + K_{a1}(d_1)^2\varphi_1 \\ &+ C_{a1}(d_1)^2\dot{\varphi}_1] \\ &-[K_{a2}(Z_{a2}-Z_{b2})c_1 \\ &+ C_{a2}(\dot{Z}_{a2}-\dot{Z}_{b2})c_1 \\ &+ F_{lm2}(c_1) + K_{a2}(c_1)^2\varphi_1 \\ &+ C_{a2}(c_1)^2\dot{\varphi}_1] \\ &+[K_{a3}(Z_{a3}-Z_{b3})(d_1) \\ &+ C_{a3}(\dot{Z}_{a3}-\dot{Z}_{b3})(d_1) \\ &+ F_{lm3}(d_1) - K_{a3}(d_1)^2\varphi_1 \\ &- C_{a3}(d_1)^2\dot{\varphi}_1] \\ &-[K_{a4}(Z_{a4}-Z_{b4})(c_1) \\ &+ C_{a4}(\dot{Z}_{a4}-\dot{Z}_{b4})(c_1) \\ &+ F_{lm4}(c_1) - K_{a4}(c_1)^2\varphi_1 \\ &- C_{a4}(c_1)^2\dot{\varphi}_1] \end{aligned} \tag{23}$$

$$\begin{aligned} I_{yy}\ddot{\theta}_2 = &[K_{a1}(Z_{a1}-Z_{b1})a_2 + C_{a1}(\dot{Z}_{a1}-\dot{Z}_{b1})a_2 \\ &- F_{lm1}(a_2) - K_{a1}(a_2)^2\theta_2 \\ &- C_{a1}(a_2)^2\dot{\theta}_2] \\ &+[K_{a2}(Z_{a2}-Z_{b2})a_2 \\ &+ C_{a2}(\dot{Z}_{a2}-\dot{Z}_{b2})a_2 \\ &- F_{lm2}(a_2) - K_{a2}(a_2)^2\theta_2 \\ &- C_{a2}(a_2)^2\dot{\theta}_2] \\ &+[-K_{a3}(Z_{a3}-Z_{b3})(b_2) \\ &- C_{a3}(\dot{Z}_{a3}-\dot{Z}_{b3})(b_2) \\ &+ F_{lm3}(b_2) - K_{a3}(b_2)^2\theta_2 \\ &- C_{a3}(b_2)^2\dot{\theta}_2] \\ &+[-K_{a4}(Z_{a4}-Z_{b4})(b_2) \\ &- C_{a4}(\dot{Z}_{a4}-\dot{Z}_{b4})(b_2) \\ &+ F_{lm4}(b_2) - K_{a4}(b_2)^2\theta_2 \\ &- C_{a4}(b_2)^2\dot{\theta}_2] \end{aligned} \tag{24}$$

$$\begin{aligned} I_{xx}\ddot{\varphi}_2 = &[-K_{a1}(Z_{a1}-Z_{b1})d_2 \\ &- C_{a1}(\dot{Z}_{a1}-\dot{Z}_{b1})d_2 \\ &+ F_{lm1}(d_2) - K_{a1}(d_2)^2\varphi_2 \\ &- C_{a1}(d_2)^2\dot{\varphi}_2] \\ &+[K_{a2}(Z_{a2}-Z_{b2})c_2 \\ &+ C_{a2}(\dot{Z}_{a2}-\dot{Z}_{b2})c_2 \\ &- F_{lm2}(c_2) - K_{a2}(c_2)^2\varphi_2 \\ &- C_{a2}(c_2)^2\dot{\varphi}_2] \\ &+[-K_{a3}(Z_{a3}-Z_{b3})(d_2) \\ &- C_{a3}(\dot{Z}_{a3}-\dot{Z}_{b3})(d_2) \\ &+ F_{lm3}(d_2) - K_{a3}(d_2)^2\varphi_2 \\ &- C_{a3}(d_2)^2\dot{\varphi}_2] \\ &+[K_{a4}(Z_{a4}-Z_{b4})(c_2) \\ &+ C_{a4}(\dot{Z}_{a4}-\dot{Z}_{b4})(c_2) \\ &- F_{lm4}(c_2) - K_{a4}(c_2)^2\varphi_2 \\ &- C_{a4}(c_2)^2\dot{\varphi}_2] \end{aligned} \tag{25}$$

Other parameters used in the simulation process are as follows:

$$Z_{a1} = -(a_2)\theta_2 + (d_2)\varphi_2 + Z_a \tag{26}$$

$$\dot{Z}_{a1} = -(a_2)\dot{\theta}_2 + (d_2)\dot{\varphi}_2 + \dot{Z}_a \tag{27}$$

$$Z_{a2} = -(a_2)\theta_2 - (c_2)\varphi_2 + Z_a \tag{28}$$

$$\dot{Z}_{a2} = -(a_2)\dot{\theta}_2 - (c_2)\dot{\varphi}_2 + \dot{Z}_a \tag{29}$$

$$Z_{a3} = b_2\theta_2 + d_2\varphi_2 + Z_a \tag{30}$$

$$\dot{Z}_{a3} = b_2\dot{\theta}_2 + d_2\dot{\varphi}_2 + \dot{Z}_a \tag{31}$$

$$Z_{a4} = b_2\theta_2 - c_2\varphi_2 + Z_a \tag{32}$$

$$\dot{Z}_{a4} = b_2\dot{\theta}_2 - c_2\dot{\varphi}_2 + \dot{Z}_a \tag{33}$$

After obtaining the dynamic equations of a passive suspension system in an ambulance with active isolated patient compartment, the open-loop state space form will be as follows:

$$\dot{X}(t) = Ax(t) + Bu(t) + B_d d(t)$$
$$Y(t) = Cx(t) + Du(t) \quad (34)$$

In the state space method, A is the system matrix (n×n), B is the matrix of actuator input into the active isolated patient compartment (n×m), Bd is the matrix of road disturbance input into the wheels (n×m), and C is the output matrix (r×m). According to 10 dynamic equations resulting from the suspension system and the active isolated patient compartment, we will have 20 stale variables, (r=10, m=4, n=20). Defining the state variables of active isolated patient's compartment: $X_1=Z_{w1}$, $X_2=\dot{Z}_{w1}$, $X_3=Z_{w2}$, $X_4=\dot{Z}_{w2}$, $X_5=Z_{w3}$, $X_6=\dot{Z}_{w3}$, $X_7=Z_{w4}$, $X_8=\dot{Z}_{w4}$, $X_9=Z_b$, $X_{10}=\dot{Z}_b$, $X_{11}=Z_{pc}$, $X_{12}=\dot{Z}_{pc}$, $X_{13}=\theta_1$, $X_{14}=\dot{\theta}_1$, $X_{15}=\varphi_1$, $X_{16}=\varphi\square_1$, $X_{17}=\theta_2$, $X_{18}=\dot{\theta}_2$, $X_{19}=\varphi_2$, $X_{20}=\varphi\square_2$.

Defining of the System outputs for active isolated patient's compartment: $Y_1=X_9$, $Y_2=X_{10}$, $Y_3=X_{11}$, $Y_4=X_{12}$, $Y_5=X_{17}$, $Y_6=X_{18}$, $Y_7=X_{19}$, $Y_8=X_{20}$.

The state space equations of active isolated patient's compartment: $\dot{X}_1 = X_2, \dot{X}_2 = \ddot{Z}_{w1}, \dot{X}_3 = X_4, \dot{X}_4 = \ddot{Z}_{w2}, \dot{X}_5 = X_6, \dot{X}_6 = \ddot{Z}_{w3}, \dot{X}_7 = X_8, \dot{X}_8 = \ddot{Z}_{w4}, \dot{X}_9 = X_{10}, \dot{X}_{10} = \ddot{Z}_b, \dot{X}_{11} = X_{12}, \dot{X}_{12} = \ddot{Z}_{pc}, \dot{X}_{13} = X_{14}, \dot{X}_{14} = \ddot{\theta}_1, \dot{X}_{15} = X_{16}, \dot{X}_{16} = \ddot{\varphi}_1, \dot{X}_{17} = X_{18}, \dot{X}_{18} = \ddot{\theta}_2, \dot{X}_{19} = X_{20}, \dot{X}_{20} = \ddot{\varphi}_2$ and Finally Matrices A, B, Bd and C are obtained through the state space equations.

4.1. Investigation of the Suspension System Stability with Active Isolated patient's compartment

Systems stability is always dependent on the location of their transfer function's poles, G(s). In the state space model of the system, the special values of the matrix A are the transfer function's poles, G(s). In order to examine the stability of the system in the state space, the eigenvalues of matrix A need to be specified. These values are either real or complex conjugate. When even one single point of the eigenvalues of matrix A stands in the right side of the imaginary axis, the system is unstable.

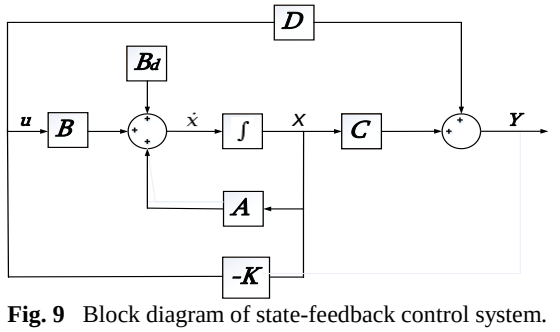

Fig. 9 Block diagram of state-feedback control system.

According to the above-mentioned and the orders in the MATLAB software. Four values of matrix A stand in the right side of the imaginary axis and the instability of the system can be definitely attributed to these values. By enforcing the control law, the poles can be steered to the proper location to stabilize the system.

As it is evident from "Fig. 9", K is the state feedback gain (m×n). After obtaining the open-loop system poles, some design processes were conducted in order to specify appropriate poles.

Finally, the appropriate poles were obtained. The matrix of feedback K (for the multi-input system) is determined in a way that it can place the closed-loop system poles in their proper position in accordance with U(t)= -K×x(t). Obviously, matrix K is not unique in the multi-input systems. In the passive suspension system, the previously obtained results were considered important because the stretcher was on a patient's compartment in which the compartment and the vehicle body were not isolated and any vertical acceleration or displacement induced by road roughness was directly transferred to the patient. Therefore, the study of the accelerations and displacements that the active isolated compartment is exposed to is of vital importance because the stretcher is directly attached to the compartment.

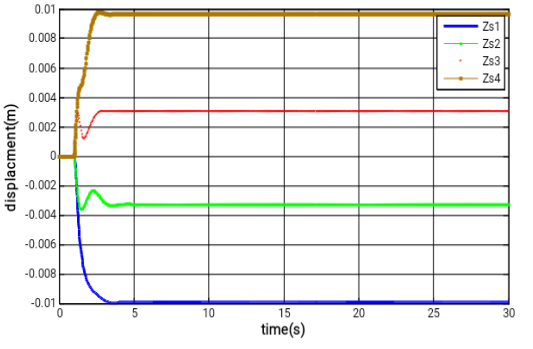

(a)

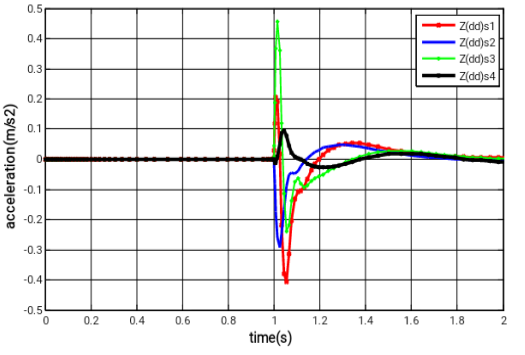

(b)

Fig. 10 The response of the passive suspension system of the ambulance with isolated patient's compartment to the step input: (a): vertical displacement, and (b): vertical acceleration.

According to diagrams in "Figs. 10-11" and "Table 4", the results are obtained from re-examination of widely-used step and Watt profile inputs in the passive suspension system with active isolated compartment. Due to the step input diagram in "Fig. 10b", the acceleration that the patients are exposed to ranges from -0.4 to +0.4 m/s² that stands within the "a little uncomfortable". In "Fig. 10a", the greatest displacement for the AVl systems ranges from -0/01 to +0/01 m and its setting time is less than 3 seconds. Also, according to the Watt profile input diagram in "Fig. 11b", the acceleration that the patients are exposed to ranges from -0.017 to +0.018 m/s² that stands within the "Not uncomfortable". In "Fig. 11a", the greatest displacement for the AVl systems ranges from -0/013 to +0/013 m and its setting time is less than 5 seconds.

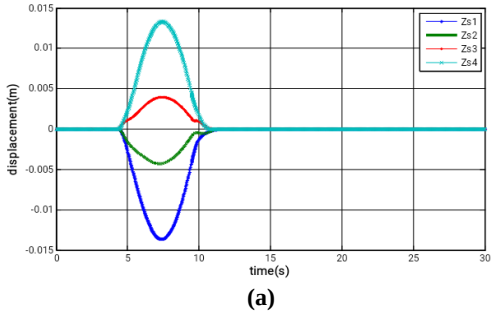

(a)

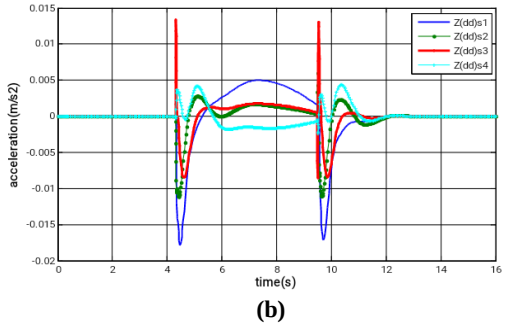

(b)

Fig. 11 The response of the passive suspension system of the ambulance with isolated patient's compartment to the watt profile input: (a): vertical displacement, and (b): Vertical acceleration.

5 ADAPTIVE CONTROL DESIGN

Adaptive control is an adjustment mechanism that sets controller parameters in real-time and Model Reference Adaptive Control (MRAC) is a model reference that provides ideal behavior of the control system [16-17]. This controller consists of an adjustable parameter and a mechanism for goal setting. The model reference adaptive control is used in the present study, in other words, the system's behavior is determined by a model and the control parameters are set according to errors. Error is the difference between the outputs of the closed-loop system and the model reference. In this system, first a control law is specified and then an appropriate Lyapunov function is selected by obtaining the equation associated with the error between the model reference and the suspension system with active isolated compartment and the control parameters are estimated in such a way that the Lyapunov function derivative is always negative. Therefore, the error signal around the origin will have asymptotic stability and the active system will comply with the model reference. Utilization of stable MRAC system as linear system through the Lyapunov theory takes place in 3 stages; 1: Identification of control structure, 2: Obtaining the error equation, 3: Identification of a Lyapunov function for obtaining the parameter updating law and making errors approach zero.

5.1. The Full-State Feedback Linearization Technique Coupled with the Adaptive Control Method

This technique will not be effective against noise when it is applied alone, but it has proved to be effective when coupled with adaptive control method. Assuming that the motion equation is as follows, we will have:

$$T = H(q)\ddot{q} + C(q.\dot{q})\dot{q} + G(q) \quad (35)$$

Assuming that:

$$C(q.\dot{q})\dot{q} + G(q) = h(q.\dot{q}) \quad (36)$$

$$C(q.\dot{q})\dot{q} = V(q.\dot{q}) \quad (37)$$

$$H^{-1}T = \ddot{q} + H^{-1}h \quad (38)$$

$$\ddot{q} = H^{-1}[T\text{-}h] = u \quad (39)$$

We will have:

$$T = Hu + h = H(q)u + h(q.\dot{q}) \quad (40)$$

Where u selected as follows:

$$u = \ddot{q_d} - K_d\tilde{\dot{q}} - K_p\tilde{q} \quad (41)$$

$$K_p = diag[\lambda_1^2.\lambda_2^2.\lambda_3^2.\ldots\lambda_n^2] \quad (42)$$

$$K_d = diag[2\lambda_1^2.2\lambda_2^2.2\lambda_3^2.\ldots 2\lambda_n^2] \quad (43)$$

$\boldsymbol{\lambda}$ shows the normal frequency of the system and any rise in their $\boldsymbol{\lambda}$ value can lead to increased velocity of the system.

$$H\left[\ddot{q_d} - K_d\tilde{\dot{q}} - K_p\tilde{q}\right] + h = H\ddot{q} + h \quad (44)$$

$$\ddot{q} - \ddot{q_d} + K_d\tilde{\dot{q}} + K_p\tilde{q} = 0 \quad (45)$$

$$\ddot{\tilde{q}} + K_d\dot{\tilde{q}} + K_p\tilde{q} = 0 \quad (46)$$

Thus, we have:

$$[M][\ddot{q}] + [C][\dot{q}] + [K][q] = [f] \quad (47)$$

According to "Eq. (47)" , $\ddot{q}$, $\dot{q}$ and q are the same as ẍ , ẋ and x. Therefore, the system state equations are transformed to the "Eq. (47)" . The mass and moments of inertia matrix $[M]$ is a 10×10 matrix that is equivalent to matrix *H*. The damping *[C]* and stiffness *[K]* matrices are also 10×10 and $[C][\dot{q}] + [K][q]$ is equivalent to $h(q.\dot{q})$ ("Fig. 12").

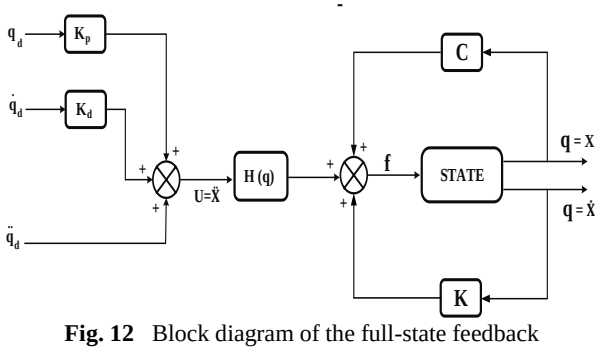

Fig. 12 Block diagram of the full-state feedback linearization technique.

In case we rewrite the Lyapunov function as follows:

$$V(x.\tilde{p}) = x^T P\, x + \tilde{p}^T \Gamma^{-1}\tilde{p} \quad (48)$$

Such that:

$$\tilde{P} = P - \hat{P} \quad (49)$$

$$\dot{\tilde{p}} = -\dot{\hat{p}} \quad (50)$$

$$A^T P + PA = -Q \quad (51)$$

$\hat{P}$ Denotes the system estimation parameters, *P* indicates the integer system parameters, and *A* is the system matrix in the state space model of the system. Assuming that Γ = diag [γ□ γ□ … γ□], $\gamma_i > 0$, it can be argued that both sentences of function *V* are non-negative and we have *V*>0.
Now we can calculate $\dot{V}$:

$$\dot{V} = \dot{X}^T PX + X^T P\dot{X} + 2\tilde{P}^T T^{-1}\dot{\tilde{P}} \quad (52)$$

$$\begin{aligned}\dot{V} &= [AX + B\hat{H}^{-1}K\tilde{P}]^T PX \\ &\quad + X^T P\left[AX + B\hat{H}^{-1}K\tilde{P}\right] \\ &\quad + 2\tilde{p}^T\Gamma^{-1}\tilde{p} \\ &= X^T A^T PX + X^T PAX + 2\tilde{p}^T\Gamma^{-1}\tilde{p} \\ &\quad + (B\hat{H}^{-1} + K\tilde{P})^T PX \\ &\quad + X^T PB\hat{H}^{-1}K\tilde{P} \\ &= X^T(A^T P + PA)X + 2\tilde{p}^T\Gamma^{-1}\tilde{p} \\ &\quad + 2\tilde{p}^T K^T\hat{H}^{-1}B^T PX\end{aligned} \quad (53)$$

Where:

$$\hat{H}^{-1^T} = \hat{H}^{-1} \quad (54)$$

$$PX = yB^T \quad (55)$$

$$B^T P = C\,.B^T PX = y \quad (56)$$

Finally, we have:

$$\dot{V} = X^T(-Q)X + 2\tilde{p}^T\left(\Gamma^{-1}\dot{\tilde{p}} + K^T\hat{H}^{-1}CX\right) \quad (57)$$

For stability, in case $2\tilde{p}^T\left(\Gamma^{-1}\dot{\tilde{p}} + K^T\hat{H}^{-1}CX\right)$ is equal to zero, then we have $\dot{V} < 0$.
Hence, the adaptive law will be as follows:

$$\dot{\hat{P}} = \Gamma K^T\hat{H}^{-1}y \quad (58)$$

Where, *K* is the system state matrix that covers [ẍ ẋ x] and *P* denoted the system parameters and Γ is a square-diagonal matrix ("Fig. 13").

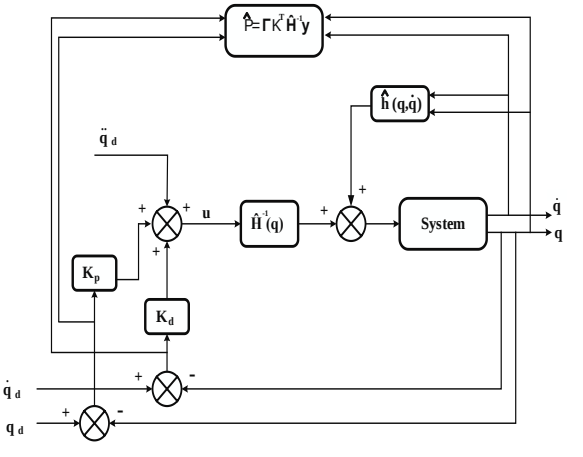

Fig. 13 Block diagram of the system's adaptive control.

5.2. Simulation and Evaluation of Responses

Any increases in the patient compartment weight and changes in the center of gravity can affect the control system. In fact, the weight variations are the changes that the system dynamics experience in reality. Model Reference is a new system that incorporates some environmental changes. Attempts will be made, by designing an adaptive controller, to have the difference between system output and optimal output (model reference output) approach zero and help the estimator track the state vector in the presence of disturbances and uncertainties so that the controller parameters can be set according to errors.

Assuming that another individual (e.g., a specialist) is present in the patient compartment together with the patient and paramedics, the patient compartment center of gravity and moments of inertia, as well as the distance between the centers of gravity and AVI systems will undergo some changes. Thus, the new data obtained from introducing the new weights into the simulation software are presented in "Table 5" .

Table 5 The new patient's compartment data after increase in the weights

Parameters	Unit	Value
Mpc	(kg)	1183
Ixx	(kg.m²)	29267.15
Iyy	(kg.m²)	29267.15
α_2	(m)	1.44
b_2	(m)	1.5147
c_2	(m)	0.6818
d_2	(m)	0.7444

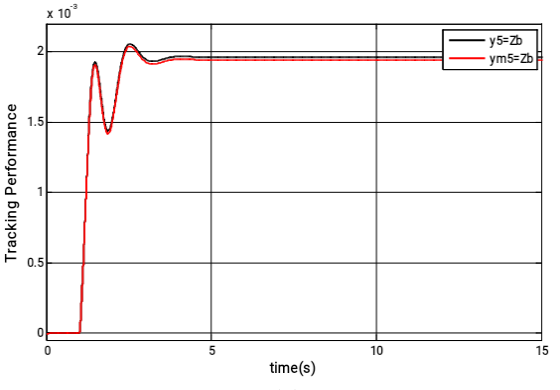

(a)

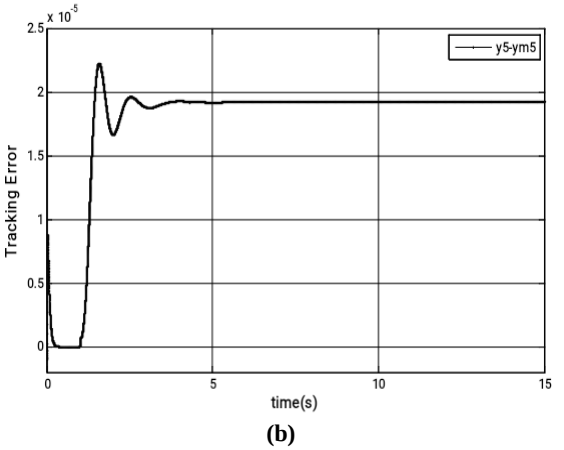

(b)

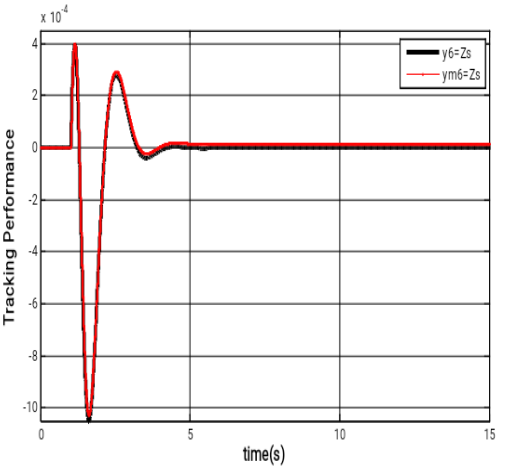

(c)

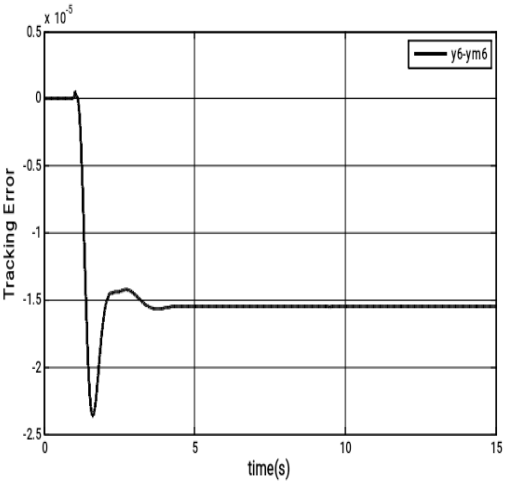

(d)

Fig. 14 (a): Tracking performance in *Zb*, (b): tracking error in *Zb*, (c): tracking performance in *Zpc*, and (d): tracking error in *Zpc*, with Step disturbance input.

The Simulink model of adaptive controller and adaptation parameters are developed according to "Fig. 13", and the model reference is developed when the road disturbance inputs such as step and watt profile are introduced to the system, and the patient compartment design data are modified according to "Table 5" .
Finally, the tracking performance and performance error of the model are investigated. The results obtained from introduction of road disturbance inputs such as step and watt are presented in "Figs. 14-15" .

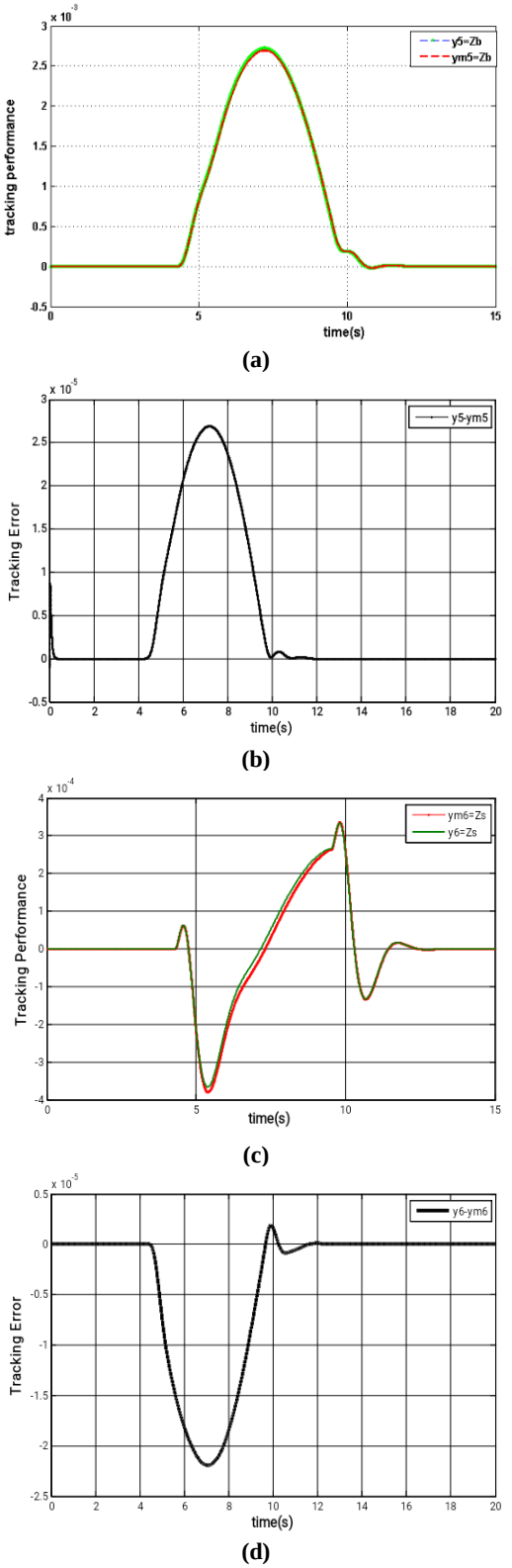

Fig. 15 (a): Tracking performance in *Zb*, (b): tracking error in *Zb*, (c): tracking performance in *Zpc*, and (d): tracking error in *Zpc*, with Watt disturbance input.

According to "Figs. 14-15" , the estimator has managed to track the state vector in the presence of disturbance and make the tracking error approach zero at the same time.

6 COUCLUSIONS

The greatest human body sensitivity to vibration stands within the 0.1 to 80 Hz and most of these vibrations are vertical. ISO 2631 standard describes extend of human comfort and discomfort when experiencing vertical acceleration. In section 3, attempts were made to investigate different inputs and their impact on passive ambulance body. Analysis of different outputs such as changes in the centre of gravity and the four corner of patient compartment that were attached to the ambulance body, showing that the diagrams setting time is considerable and the diagrams (especially the acceleration diagram) stand in the uncomfortable range. The performance of diagrams was also confirmed based on the experimental observation and various reports. Active vibration isolator system in the present study mainly refers to a system that can reduce the vertical forces and vibrations that the patient and paramedics are exposed to through isolation of patient's compartment from passive suspension system of ambulances.

Hence, the active vibration isolator system that is also known as AVI was designed for this purpose. Using the pneumatic and electromagnetic forces used in its design, this system is able to significantly attenuate the vertical vibrations exerted to the ambulance body or to the patient's body. The adaptation parameters are developed by means of the control law, the model reference adaptive controller, and the acceleration sensors that measure the road disturbance signals serving as controller feedback, and finally the obtained values with optimal values were compared. Moreover, the model reference adaptive controller allows for integrated control of AVI system in the full-scale ambulance vehicle. Evaluation of the acceleration output diagram and comparison of that with passive state when the step input is introduced to the system as road disturbance, show that the acceleration has declined by over 90% and patient discomfort scale presented in "Table 4" , will change from "extremely uncomfortable" to "a little uncomfortable".

As for displacement, the active isolated system, as compared to the passive suspension system, has managed to reduce displacements by 80%, similarly, in the watt profile road disturbance input, the vertical acceleration has changed from "a little uncomfortable" to "not uncomfortable" that is indicate of the attenuation of acceleration by 96%.

7 NOMENCLATURES

K_a	Air springstiffness (N/m)
γ	Specific heat ratio of air spring
A_c	Effective air spring area (m^2)
p_0	Pressure difference between the internal pressure of the air spring and the ambient pressure (Pa)
V_0	Volume of the air spring (m^3)
f_n	Resonance frequency (Hz)
E	Modulus of elasticity (GPa)
Mt	Ambulance mass (Kg)
Mb	Mass ambulance without patient's compartment (Kg)
Mpc	Mass of the patient's compartment (Kg)
Kb	Spring stiffness coefficient (kN/m)
Cb	Spring damping coefficient (Ns/m)
Ca	Air spring damping coefficient (Ns/m)
Mw	Wheel mass (Kg)
Z	Vertical displacement (m)
F_{lm}	Force of the linear shaft motor (N)
I	Moment of inertia (kg.m²)

Greek symbols

ø	Roll-the rotation of a vehicle about the longitudinal axis
θ	Pitch-the rotation of a vehicle about the transverse axis

State space model symbols

A	State (or system) matrix (n×n)
B	Input matrix (n×m)
C	Output matrix (r×n)
D	Feedforward matrix (zero matrix) (r×m)
Bd	Road-to-wheel disturbance input matrix (n×m)

Adaptive Control symbols

$[f]$	Matrix of the control forces that is equivalent to T
$[M]$	Symmetric mass matrix that is equivalent to H(q)
$[C]$	Damping matrix that is equivalent to C(q. q̇)
$[K]$	Stiffness matrix
$h(q.\dot{q})$	Equivalent to$[C][\dot{q}] + [K][q]$
q	System displacement variable that is equivalent to x
$\dot{q}$	System velocity variable that is equivalent to ẋ
$\ddot{q}$	System acceleration variable that is equivalent to ẍ
λ	Normal frequency of the system
$\hat{P}$	System estimation parameters
P	The integer system parameters
K	System state matrix that covers [ẍ ẋ x]
Γ	Square-diagonal matrix.

REFERENCES

[1] Chung, T. N., Kim, S. W., Cho, Y. S., Chung, S. P., Park, I., and Kim, S. H., Effect of Vehicle Speed on The Quality of Closed-Chest Compression During Ambulance Transport, Resuscitation, Vol. 81, No. 7, 2010, pp. 841-847.

[2] Browning, J., Walding, D., Klasen, J., and David, Y., Vibration Issues of Neonatal Incubators During in-Hospital Transport, Journal of Clinical Engineering, 2008, pp.74-77.

[3] Blaxter, L., Yeo, M., McNally, D., Crowe, J., Henry, C., Hill, S., Mansfield, N., Leslie, A., and Sharkey, D., Neonatal Head and Torso Vibration Exposure During Inter-Hospital Transfer, Proceedings of the Institution of Mechanical Engineers, Part H: Journal of Engineering in Medicine, Vol. 231, No. 2, 2017, pp. 99–113, doi: 10.1177/0954411916680235.

[4] Karlsson, B. M., Lindkvist, M., Lindkvist, M., Karlsson, M., Lundström, R., Håkansson, S., Wiklund, U., and Van den Berg, J., Sound and Vibration: Effects on Infants' Heart Rate and Heart Rate Variability During Neonatal Transport, Acta paediatrica, 2012, doi:10.1111/j.1651-2227.2011.02472.x.

[5] Shintani, M., Hirai, Y., Ogawa, Y., Study on Two-Dimensional Base-Isolating Device for Sick Person's Bed in Ambulance, In 2012 Proceedings of SICE Annual Conference (SICE), 2012, pp. 225-231, IEEE.

[6] Abd-El-Tawwab, A. M., Ambulance Stretcher with Active Control Isolator System, Journal of Low Frequency Noise, Vibration and Active Control, Vol. 20, No. 4, 2001, pp. 217-27.

[7] Chae, H. D., Choi, S. B., A New Vibration Isolation Bed Stage with Magnetorheological Dampers for Ambulance Vehicles, Smart Materials and Structures, Vol. 24, No. 1, 2014, pp. 017001.

[8] Henderson, R. J., Raine, J. K., A Two-Degree-of-Freedom Ambulance Stretcher Suspension, Part 2: Simulation of System Performance with Capillary and Orifice Pneumatic Damping, Proceedings of the Institution of Mechanical Engineers, Part D: Journal of Automobile Engineering, Vol. 212, No. 3, 1998, pp. 227-40.

[9] Raemaekers, A., Active Vibration Isolator Design for Ambulance Patients, Eindhoven: Eindhoven University of Technology, 2009.

[10] Fu, N., Wenjuan, W., Jinggong, S., Xudong, R., Chen, S., Lingshuai, M., and Hongyan, J., Experimental Investigation of An Ambulance Stretcher Suspension Using Spring and Metal Rubber Structure, In The 22nd International Congress on Sound and Vibration, Florence, Italy 2015.

[11] Chae, H. D., Choi, S. B., A New Vibration Isolation Bed Stage with Magnetorheological Dampers for Ambulance Vehicles, Smart Materials and Structures, Vol. 24, No. 1, 2014, pp. 017001.

[12] Qi, H., Zhang, N., Chen, Y., and Tan, B., A Comprehensive Tune of Coupled Roll and Lateral Dynamics and Parameter Sensitivity Study for A Vehicle Fitted with Hydraulically Interconnected Suspension System, Proceedings of The Institution of Mechanical Engineers, Part D: Journal of Automobile Engineering, 2021, doi: 10.1177/0954407020944287.

[13] Fialho, I., Balas, G. J., Road Adaptive Active Suspension Design Using Linear Parameter-Varying Gain-Scheduling, IEEE Transactions on Control Systems Technology, Vol. 10, No. 1, 2002, pp. 43-54.

[14] Nguyen, A. T., Rafaq, M. S., Choi, H. H., Jung, J. W., A Model Reference Adaptive Control Based Speed Controller for A Surface-Mounted Permanent Magnet Synchronous Motor Drive, IEEE Transactions on Industrial Electronics, Vol. 65, No. 12, 2018, pp. 9399-409.

[15] Amiri, M. S., Ramli, R., and Ibrahim, M. F., Initialized Model Reference Adaptive Control for Lower Limb Exoskeleton, IEEE Access, Vol. 7, 2019, pp. 167210-20.

[16] Vargas-Martínez, A., Garza-Castañón, L. E., Puig, V., and Morales-Menéndez, R., Robust MRAC-Based Fault Tolerant Control for Additive and Multiplicative Faults in Nonlinear Systems, IFAC Proceedings Volumes, Vol. 45, No. 20, 2012, pp. 540-5.

[17] Nair, A. P., Selvaganesan, N., and Lalithambika, V. R., Lyapunov Based PD/PID in Model Reference Adaptive Control for Satellite Launch Vehicle Systems, Aerospace Science and Technology, Vol. 51, 2016, pp. 70-7.